Control of humanoid robot motions with impacts
Numerical experiments with reference spreading control

Rijnen, Mark; De Mooij, Eric; Traversaro, Silvio; Nori, Francesco; Van De Wouw, Nathan; Saccon, Alessandro; Nijmeijer, Henk

DOI
10.1109/ICRA.2017.7989472

Publication date
2017

Document Version
Final published version

Published in
Proceedings 2017 IEEE International Conference on Robotics and Automation (ICRA)

2017 IEEE International Conference on Robotics and Automation (ICRA)
Singapore, May 29 - June 3, 2017

Control of Humanoid Robot Motions with Impacts: Numerical Experiments with Reference Spreading Control

Mark Rijnen[1], Eric de Mooij[1], Silvio Traversaro[2], Francesco Nori[2], Nathan van de Wouw[1], Alessandro Saccon[1], and Henk Nijmeijer[1]

Abstract— **This work explores the stabilization of desired dynamic motion tasks involving hard impacts at non-negligible speed for humanoid robots. To this end, a so-called reference spreading hybrid control law is designed showing promising results in simulation. The simulations are performed employing a dynamical model of an existing humanoid robot and impacts are assumed to be inelastic. The desired motion task consists of having the robot balancing on one foot while repeatedly making and breaking contact with a wall by means of one hand. The simulation results illustrate that the considered controller is suited to control humanoid robot motions with impacts.**

I. Introduction

Performing locomotion and manipulation tasks at relative high speed still poses many challenges to a robotic system. Besides the limitations represented by the current mechanical structures and the challenges in perception and actuation design, another limitation derives from the still limited number of control algorithms specifically designed to reach the theoretically achievable optimal performance.

Trajectory tracking control for hybrid systems with state jumps is an active field of research in the control community [1]–[5] and has a relatively long history (see, e.g., [6] and references therein). Robotic systems performing locomotion and manipulation tasks involving contact can be modeled as hybrid systems (see, e.g., [7]) where the state jumps correspond to the rapid velocity changes occurring in making contact with the environment. Since the velocity jumps occur only when the robot gets in contact with the environment, the velocity jumps are state triggered. In the control of hybrid systems with state-triggered jumps, it cannot be assumed that the impact times of the controlled robot coincide with those of the planned desired motion. To deal with this time mismatch, different authors have proposed different notions of tracking error [2]–[5]. These error definitions are required for comparing the current state of the robot with the desired state, in particular whenever the robot experiences the impact before the planned desired motion or vice versa.

[1]M.W.L.M. Rijnen, E.B.C. de Mooij, N. van de Wouw, A. Saccon, and H. Nijmeijer are with the Department of Mechanical Engineering, Eindhoven University of Technology, 5600MB Eindhoven, The Netherlands (e-mail: m.w.l.m.rijnen@tue.nl; eric.de.mooij@hotmail.com; n.v.d.wouw@tue.nl; a.saccon@tue.nl; h.nijmeijer@tue.nl). N. van de Wouw is furthermore with the Department of Civil, Environmental and Geo-Engineering, University of Minnesota, MN 55455 Minneapolis, USA, and with the Delft Center for Systems and Control, Delft University of Technology, 2628CD Delft, The Netherlands.

[2]S. Traversaro and F. Nori are with the iCub facility at the Istituto Italiano di Tecnologia, 16163 Genoa, Italy (e-mail: Silvio.Traversaro@iit.it; Francesco.Nori@iit.it).

In this paper, we employ the error definition presented in [4] and apply it to stabilize a desired motion task for a humanoid robot. The control strategy that emerges from employing this specific tracking error definition has been termed reference spreading hybrid control [4], [8]–[10]. Generally speaking, reference spreading allows for dealing with aperiodic desired trajectories and contact transitions due to elastic and inelastic impacts. Here we focus just on the inelastic case.

Recent literature on humanoid robot control has focused on the synthesis of complex multi-contact behaviors from several possibly conflicting tasks while ensuring to balance the robot: see, e.g., [11]–[15] and references therein. These task-based optimal constrained controllers are able to generate impressive motions and have been demonstrated on real robots. The underlying assumption is however that either the set of contact constraints remain the same or, when contact is made or broken, this either happens at negligible speed or the robot compliance is sufficient to stabilize the contact transition: once an equilibrium has been reached, the controller then switches to a set of new tasks and constraints, sometimes using blending functions to avoid control torque jumps. Exception of these general assumptions is represented, in particular, by [7] and [16] where impact phenomena are directly modeled and taken into account in the design of the control strategy, although the theoretical foundation is currently limited to stabilization of periodic motions and, in particular, to walking and running gaits. There is therefore a theoretical gap that needs to be filled in enabling the execution of generic dynamic motions that include the sudden velocity variations due to impacts at medium and relatively high speed (as, for example, those computed with numerical optimal control algorithms in [17]).

The main contribution of this paper is the demonstration that reference spreading hybrid control can be used to stabilize a humanoid robot's desired motion in performing contact tasks involving impacts. We employ the humanoid robot iCub [13] as a benchmark robotic system to test the reference spreading hybrid control. We present a simulation study using a dynamic model of the humanoid robot iCub stabilizing an impacting reference trajectory where the robot is standing on one foot and reaches towards a wall with its hand. After an impact between wall and hand (at non-negligible speed of 0.23 $\mathrm{m/s}$), the robot pushes itself away from the wall and returns back to its initial posture and repeats this 'single-hand horizontal push-up' motion.

This paper is organized as follows. In Section II, we discuss the humanoid robot model and desired motion. The essentials of reference spreading hybrid control are given in Section III. In Section IV, we detail how the reference motion with impacts was generated. The results of closed-loop simulations are discussed in Section V. Conclusions are presented in Section VI.

II. Humanoid robot dynamics with impacts

To validate the reference spreading hybrid control, we have created a simulation environment starting from an available code to compute the free-floating dynamics of the humanoid robot iCub [13], and adding suitable contact detection and velocity reset maps for the intended impacting motion task.

In this research, we assume that the head degrees of freedom (DOFs) are locked and that the hands are not present, reducing the DOFs effectively employed for the motion task detailed below from 53 to 25. We write the configuration of the robot as $q := (H, q_J) \in SE(3) \times \mathbb{R}^{n_J}$, where H is the homogeneous transformation matrix describing the pose of the robot's root link with respect to the inertial frame and q_J represents the $n_J = 25$ joint variables. The generalized velocity is $\nu := (\mathrm{v}, \dot{\mathrm{q}}_{\mathrm{J}}) \in \mathbb{R}^{6+\mathrm{n_J}}$ with $\mathrm{v} \in \mathbb{R}^6$ the root link twist describing the velocity of the base with respect to the inertial frame.

The motion task we consider in this paper – further details are given in Section IV– makes use of persistent contact between the robot's left foot and the ground and intermittent contact between its left hand and a wall. To be more precise, as we have in fact no hand, one should talk about the robot's wrist, rather than its hand, but we are confident the reader will not bother with this terminology issue.

The left foot is centered at the origin of the inertial frame and the wall is positioned at a distance of $x_{wall} = 0.4$ m from the left foot center along the inertial x axis. The floor, foot, hand, and wall are all considered rigid. In our simulator, the unilateral contact constraint between the left foot and the ground is modeled as a bilateral constraint (fixing the foot's three rotations and three translations) and constraint ground-foot torques and forces are monitored online to ensure feasibility of the result (we stop the simulation if the ground starts "pulling the foot"). More precisely, the foot-ground constraint validity is monitored by checking if the zero-moment-point (ZMP) remains inside the convex hull of the foot sole and if the component of the foot contact force normal to the floor is positive. If either one of these two conditions is breached, the simulation is terminated as the contact modeling using the constraint is no longer physically valid (the ground cannot hold the foot). The hand-wall constraint is instead modeled as a unilateral constraint in the inertial x-axis, monitoring the hand-wall distance and imposing it to be always larger than, or equal to, zero.

The number of active constraints varies therefore over time and so does the continuous dynamics, depending if the hand-wall contact is closed or open. The hand transition from free motion to contact is modeled as an inelastic impact, considered as being a discrete event resulting in a jump in velocity (impulsive forces are applied). As long as the hand contact persists, static friction is assumed to be present, not allowing any in-plane motion of the hand along the wall. No state reset is necessary for the transition from constrained to free motion. The resulting dynamics model is that of a hybrid system, valid in a "neighborhood" of the intended motion task. Further details are given below.

The equations of motion for the continuous dynamics are

$$M(q)\dot{\nu} + h(q,\nu) = S\tau + J_{foot}^T(q)\ \mathrm{f}_{foot} + J_{hand}^T(q) f_{hand}, \quad (1)$$

$$J_{foot}(q)\dot{\nu} + \dot{J}_{foot}(q)\nu = 0_6, \quad (2)$$

where $M(q) \in \mathbb{R}^{n \times n}$, $n = n_J + 6$, is the mass matrix, $h(q,\nu) \in \mathbb{R}^n$ the vector of generalized bias forces, $S = \left(0_{n_J \times 6}, I_{n_J}\right)^T$ the selection matrix showing the underactuated nature of the robot, $\tau \in \mathbb{R}^{n_J}$ the joint torques, $\mathrm{f}_{foot} \in \mathbb{R}^6$ the contact wrench at the left foot, $J_{foot}(q) \in \mathbb{R}^{6 \times n}$ the Jacobian associated with the left foot contact frame, $f_{hand} \in \mathbb{R}^3$ the contact force at the left hand, and $J_{hand}(q) \in \mathbb{R}^{3 \times n}$ the Jacobian associated with the translational motion of the left hand contact point.

As the hand-wall contact is modeled as a unilateral constraint, Signorini's law [18, Section 5.4] is enforced: $0 \leq (f_{hand})_x \perp \gamma(q) \geq 0$, where $(f_{hand})_x$ denotes the component of the contact force normal to the wall and $\gamma(q) := x_{wall} - (o_{hand})_x$ the distance between hand and wall, where $(o_{hand})_x$ is the inertial x-coordinate of the origin of the left hand frame.

When $\gamma(q)$ becomes zero, the hand contact constraint becomes active and an inelastic impact occurs. For the components of f_{hand} that are tangential to the wall, a Coulomb friction model with infinite friction coefficient is also considered, therewith effectively introducing two bilateral constraints on the in-plane motion of the hand along the wall as long as the hand contact persists. Therefore, at the moment of impact, an impulsive force with magnitude $\lambda_{hand} \in \mathbb{R}^3$ is applied on the hand therewith leading to an impulsive (reaction) contact wrench with magnitude $\Lambda_{foot} \in \mathbb{R}^6$ on the foot. The velocity ν^+ just after the impact can be computed in terms of the velocity ν^- just before impact by solving the linear system

$$\begin{bmatrix} M(q) & -J_{hand}^T(q) & -J_{foot}^T(q) \\ J_{hand}(q) & 0 & 0 \\ J_{foot}(q) & 0 & 0 \end{bmatrix} \begin{bmatrix} \nu^+ \\ \lambda_{hand} \\ \Lambda_{foot} \end{bmatrix} = \begin{bmatrix} M(q)\nu^- \\ 0_3 \\ 0_6 \end{bmatrix}. \quad (3)$$

The derivation of this jump map can be found in [19, Section 2.3]. Similarly as for the foot contact wrench $\mathrm{f}_{\mathrm{foot}}$ (monitored via the ZMP condition in continuous time), Λ_{foot} is checked after applying the jump map to ensure that the foot-ground contact constraint should remain closed after the impact.

Equations (1)-(3) describe the dynamics of a hybrid system with two modes, where the discrete events are triggered based on conditions that depend on the state of the system. From here on, the modes will be referred to as *contact mode* and *free-motion mode*. In the remaining sections, we show how we generate a reference trajectory $\alpha = (q_J^d, \dot{q}_J^d)$ with impacts and then make the robot follow that time-varying reference trajectory that transitions between the free-motion and contact modes, employing reference spreading control.

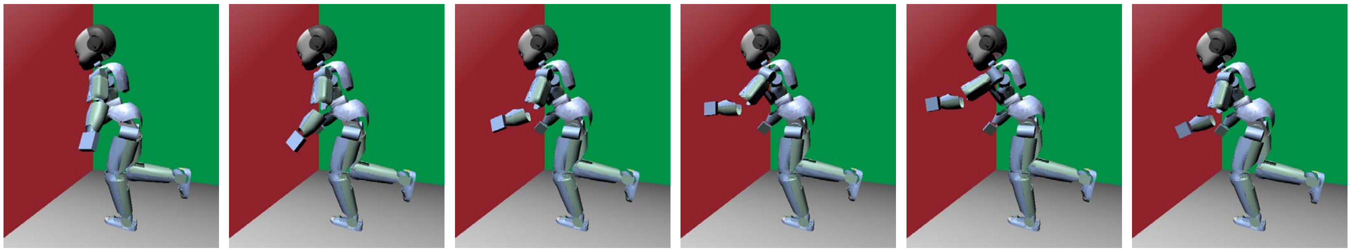

$t = 0$ s $\quad$ $t = 0.22$ s $\quad$ $t = 0.44$ s $\quad$ $t = 0.66$ s $\quad$ $t = 0.88$ s $\quad$ $t = 1.1$ s

Fig. 1: Snapshots of the reference contact task (first cycle). The hand-wall impact occurs at approximately $t = 0.7$ s.

III. Reference spreading hybrid control

Reference spreading hybrid control [4], [8] is a recently introduced strategy for tracking discontinuous trajectories of hybrid systems. It can be applied, as we demonstrate also here, to track a desired robot motion with impacts [10]. The strategy provides a solution for handling the unavoidable time mismatches between planned and closed-loop impact times that typically lead to undesired spiking control inputs and possibly poor tracking performance [3].

The key idea is to have more than one reference in a neighborhood of the nominal impact events and to appropriately switch between them. Namely, the reference trajectory α is partitioned into segments between mode switches and subsequently each segment is extended separately by forward and backwards integration of the continuous dynamics disregarding the unilateral constraints that would have triggered a state jump. Switching from one extended reference trajectory segment to the next occurs online at the detection of a closed-loop impact as opposed to at the expected time based on the nominal impact events. By doing so, the jump in velocity error occurs only when an impact occurs and no longer when the non-extended reference trajectory jumps [4], [8], [10].

Each segment of the reference is labeled using a discrete event counter $j \in \mathbb{N}$, typically referred to as the discrete time in the hybrid system literature. The extended reference trajectory comprising the different segments, one for each value of j, is denoted $\bar{\alpha}(t, j) = (\bar{q}_J^d, \dot{\bar{q}}_J^d)$. In reference spreading hybrid control, the tracking error is the difference between the extended reference and the system state at the current hybrid time (t, j). As the state for a mechanical system is naturally split in joint configuration and velocity, the control action assumes the form of a PD control with feedforward

$$\tau(t, j) = \tau^d(t, j) - K_p\, e_{q_J}(t, j) - K_d\, e_{\dot{q}_J}(t, j) \tag{4}$$

where τ^d is the feedforward input, $e_{q_J}(t, j) := q_J(t, j) - \bar{q}_J^d(t, j)$ and $e_{\dot{q}_J}(t, j) := \dot{q}_J(t, j) - \dot{\bar{q}}_J^d(t, j)$ are the joint configuration and velocity errors, and $K_p \in \mathbb{R}^{n_J \times n_J}$ and $K_d \in \mathbb{R}^{n_J \times n_J}$ are feedback gain matrices.

The gain matrices can be time-varying and may be different for each mode. They can be designed, in an optimal sense, using the hybrid linearization of the hybrid system as described in [4], [8]. This approach is however not taken in this work since computing the linearization is not yet possible for such a complex humanoid robot and therefore we only consider constant gains that are however different for the contact and free-motion modes.

The reference spreading hybrid control will be employed to track a state-input reference with jumps (α, τ^d) that is a trajectory of the system (1)-(3), complying with the constraints: in particular, having a feasible non-pulling foot contact wrench. The topic of finding such a feasible trajectory will be addressed in the next section. The closed-loop behavior will be discussed in Section V.

IV. Extended reference trajectory generation

In the following two subsections, we detail the generation of the extended reference trajectory starting from the generation of a reference trajectory with impacts and concluding with the extension of each segment composing it.

A. Reference trajectory generation from motion tasks

As mentioned in Section II, the contact task starts with the robot balancing on its left foot. The robot gradually moves itself forward reaching out with its left hand, until the hand impacts a wall in front of the robot. Once the hand makes contact with the wall, the robot pushes itself away from the wall, back to standing on one foot (with the left hand detached from the wall again). From the standing position, the robot repeats the last two steps indefinitely; reaching towards the wall, and pushing itself away again.

Six snapshots of the impact motion task are depicted in Figure 1. The snapshots are taken from the accompanying video (available at `http://ieeexplore.ieee.org`) which contains animations of the motion and furthermore illustrates the tracking results that will be discussed in Section V, also illustrating the quite large basin of attraction provided by the controller around the desired motion.

We have constructed such a reference trajectory employing an already existing task-based optimal constrained controller for humanoid robot balancing [20], [21]. A detailed explanation of the trajectory generation process for the desired motion described in this paper can be found in [19, Section 3]. Here we only provide a brief description of it.

The generation of the reference trajectory can be summarized as the execution of the following steps:

1) Two CoM and hand tasks are designed (in a trial and error fashion) to move the robot forward while also extending the left hand towards the wall. The hand task is designed with the explicit purpose of hitting the wall, not to land softly on it. The corresponding

state and input trajectory is generated solving for the constrained optimization problem on the joint torques as discussed in [20], [21];

2) Time integration is stopped when the robot hand gets in contact with the wall (the impact speed is approximately 0.23 m/s). The state is reset employing the jump map (3) and a consistency check is applied to ensure that during the impact the foot does not detach;
3) The continuous time integration is restarted from the new initial condition employing the same balancing controller where however two new tasks for the hand and the CoM are used to create a push-away motion (the hand task is the position constraint for the hand);
4) Time integration is stopped when the hand contact force normal becomes zero, signaling the transition from contact to free motion. No reset of the state is necessary (the impact map is the identity) but the hand position constraint is now removed;
5) The continuous time integration is restarted applying different tasks on the CoM and hand to move the robot back to approximately the same initial configuration and after that moving towards the wall again.

The above steps are repeated indefinitely to form a repetitive contact motion.

B. Reference trajectory extension

We employ the optimal constrained controller to generate the extensions of the reference trajectory in a neighborhood of the nominal contact and detachment times. To the best of our knowledge, this is the first time a task-based optimal constrained controlled is employed for this purpose.

The CoM and hand tasks can be easily defined forward and backward in time from the nominal event times. While the optimal constrained controller works very well for forward extensions (e.g. where the hand moves through the wall), the method is found to be inappropriate for the backwards extensions due to the instability in reverse time and the complex nature of the robot. We solved this issue by changing the sign of the feedback gains used in the controller when creating the backwards extensions. Gains are changed in a continuous manner to avoid discontinuities in the accelerations in a neighborhood of the nominal contact and detachment events, therewith stabilizing the system also in backward time. Further details are provided in [19, Section 3.3]. Note how for each segment we obtain a different reference torque input, which justifies the presence of the index counter j in the feedforward τ^d appearing in (4).

The result of the approach is a feasible state-input reference trajectory with impacts together with reference extensions that can be employed in reference spreading control.

Considering the large number of DOFs, presenting the obtained reference trajectory for each joint is out of the scope of this paper. We opted instead to report in Figure 2 only the position and velocity of the CoM and the hand with respect to the inertial frame. Note, in particular, the jumps in v_{hand} at the moments of impact (e.g. for $t = 0.7$ s). As mentioned previously, the found impact velocity is about 0.23 m/s. In

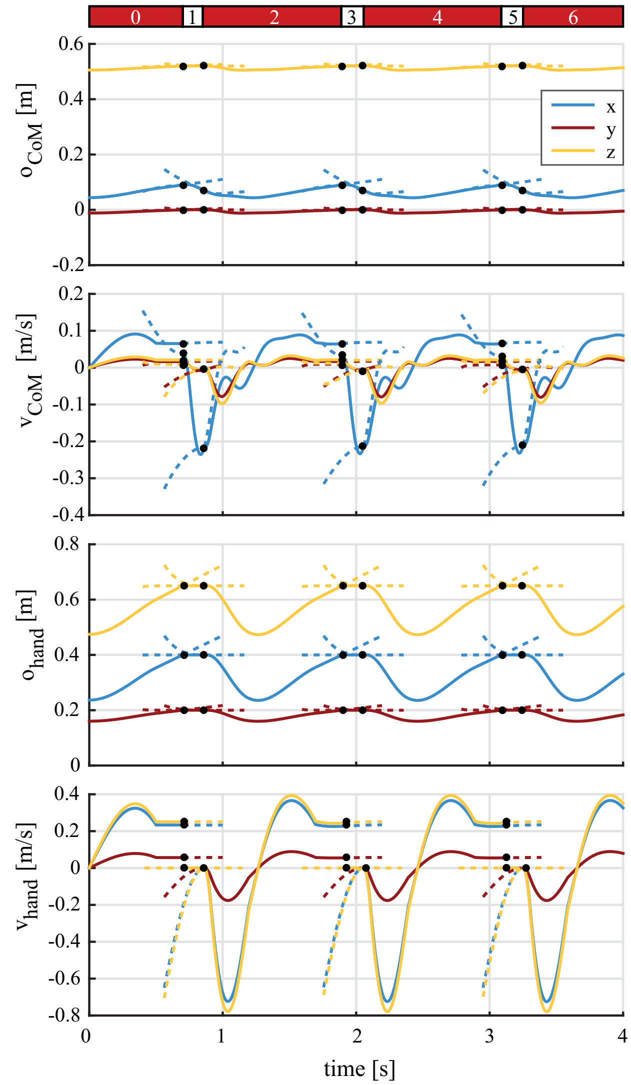

Fig. 2: Reference positions and linear velocities of the CoM and left hand w.r.t. the inertial frame (solid) with corresponding extensions (dashed). The bar on top shows the discrete time j (red = free motion, white = contact)

Figure 2, the numbered bar on top illustrates the discrete time j and the current mode (red = free motion mode, white = contact mode). The dashed lines represent the extensions.

V. Controller Tuning and Numerical Results

In this section, we use the reference spreading hybrid controller to track the reference trajectory created in Section IV. In the implementation, we stored the reference position q_J^d and velocity $\dot{q}_J^d$ for the internal joints since the pose and velocity H and v are redundant due to the persistent contact between foot and ground, basically eliminating six DOFs.

The diagonal feedback gain matrices K_p and K_d have been tuned manually, separately for each joint, based on desired convergence rates. The gains for each individual joint are designed for a joint angle error reduction of approximately 60% in 0.5 s. Subsequently, the position feedback for the left leg is increased and the velocity feedback gains for the different joints are reduced. The former is done such that the

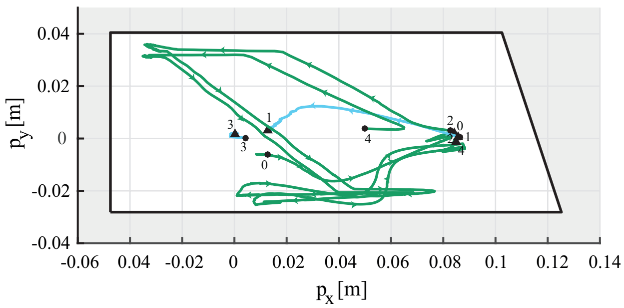

Fig. 3: The x and y coordinates of the closed-loop ZMP over time. Numbers indicate the discrete time j.

system rejects errors in its support quicker, therewith reducing the chance of it falling over, and the latter modification is to prevent the robot from reacting too strongly to the change in velocity error at impact. The tuned gains are omitted here due to space restrictions, but can be found in [19, Table 4.3]. The reader is also referred to [19, Chapter 4] for insight on the sensitivity of the tracking results to gain selection and robustness to model inaccuracies.

We randomly perturb the initial joint angles $q_J(t_0)$ from the reference initial condition in the range ± 5 degrees for the arms and right leg and ± 0.5 degrees for left leg and torso (the ranges are chosen such that, when perturbed, the robot still starts in a balanced pose). In addition to these random perturbations, we add an intended perturbation to the left arm DOFs such that it is initially farther from the wall. This induces a large difference in impact time between the closed-loop system and reference trajectory.

A trajectory tracking simulation is performed on the iCub model using a perturbed initial condition and the tuned gains as mentioned above. The resulting ZMP as a function of time is depicted in Figure 3 together with the support polygon of the robot. The color of the plot indicates that the robot is in free motion mode (dark green) or in contact mode (light blue) and the dots and triangles illustrate the start, respectively, the end of a mode. Clearly, the ZMP remains within the support polygon therewith indicating the validity of the foot contact constraint. In Figure 4, the total joint angle and velocity error norms and the norm of the actuation torque during the motion are depicted. Both error norms converge to zero over time. The figure illustrates a large jump in the velocity error norm at the impact times. This is caused by the inevitable difference between the closed-loop and reference trajectory at the closed-loop impact times. Nevertheless, the simulation indicates that the reference spreading controller successfully stabilizes the hybrid reference trajectory.

In Figure 5, the closed-loop results are mapped into the task space. The figure shows the position and velocity errors of the CoM and left hand as a function of time (expressed in the directions of the inertial frame). Since the joint angles converge to the reference trajectory (see Figure 4), these errors naturally converge to zero as well. The x-direction component of the CoM velocity error shows a large jump at the first impact time. This is most likely caused by the large mismatch in impact time and high acceleration in x-direction

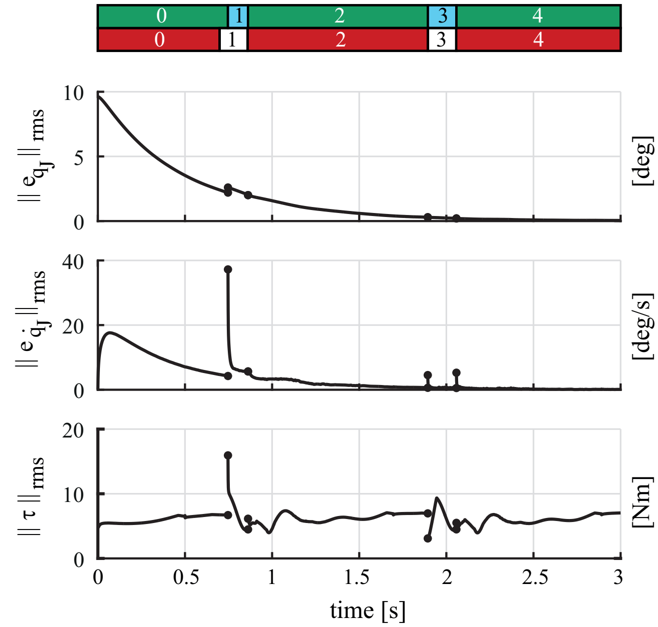

Fig. 4: Closed-loop joint angle and joint velocity error norms and actuation torques. The colored strips on top show j for the closed-loop system (the reference motion). Green (red) indicates free motion, blue (white) contact.

for the CoM of the reference just after impact (see Figure 2). In Figure 5, the x-direction components for the different errors are overall larger than those for the other directions. This is caused by the selective perturbation of the initial conditions, which mainly influences the x-coordinate of the hand (and subsequently of the CoM).

From the simulation results, it can be concluded that the reference spreading controller can effectively stabilize a reference trajectory with jumps for a humanoid robot even when the closed-loop system experiences the impact events significantly later than the reference trajectory.

VI. Conclusion

We showed by means of simulations that a reference spreading controller can successfully stabilize a humanoid robot's desired motion with impacts. We considered specifically a desired motion where the robot stands on one leg and performs a motion with its whole body resulting in its hand impacting a wall in front of it. After the inelastic impact with the wall, the robot pushes itself away from it, returns in a standing position on one foot, and repeats the hand-wall impact motion indefinitely. Although the motion we have illustrated is essentially periodic, there is no intrinsic limitation in applying the strategy to aperiodic impact motions.

We detailed the hybrid dynamical model that we employed to perform the simulations and also to generate the state-input trajectory corresponding to the desired motion. The desired trajectory with impacts has been generated employing a modification of an existing task-level optimal constrained controlled. The generated trajectory with impacts is then extended by spreading the reference beyond the nominal impact times using backward and forward time integration. The

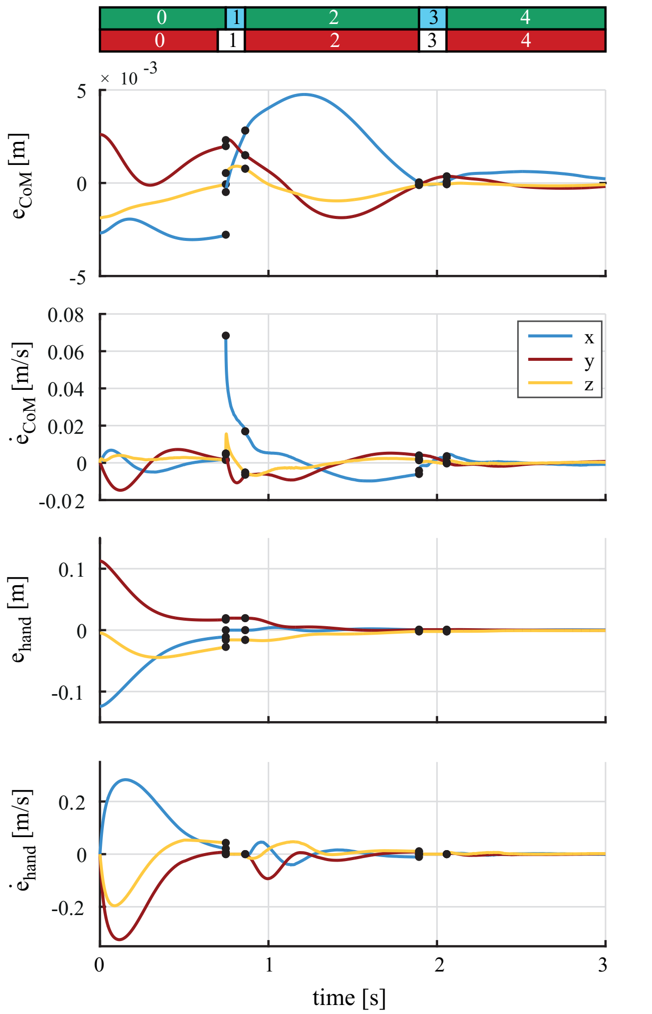

Fig. 5: Position and velocity errors for the CoM and left hand in tracking the reference trajectory. The colored strips on top show j for the closed-loop system (the reference motion). Green (red) indicates free motion, blue (white) contact.

extended trajectory is the input for the reference spreading controller, whose gains have been tuned manually. The paper illustrates that reference spreading control can be used to track trajectories with hard impacts even when other contact constraints, such as the foot constraint, are active at impact.

Our ambition is to apply the reference spreading hybrid controller on a real humanoid robot, but this clearly requires a series of intermediate steps that we are currently undertaking. Our program includes the transformation of the reference spreading strategy from a state feedback into a task-level optimal constrained controller based on extended trajectories. We are also developing an efficient algorithm to compute the jumping linearization for such a complex mechanism to allow for automatic tuning of the control gains taking into account that impacts will occur.

References

[1] S. Galeani, L. Menini, and A. Potini, "Robust trajectory tracking for a class of hybrid systems: An internal model principle approach," *IEEE Transactions on Automatic Control*, vol. 57, no. 2, pp. 344–359, 2012.

[2] F. Forni, A. R. Teel, and L. Zaccarian, "Follow the bouncing ball: global results on tracking and state estimation with impacts," *IEEE Transaction on Automatic Control*, vol. 58, no. 6, pp. 1470–1485, 2013.

[3] J. J. B. Biemond, N. van de Wouw, W. P. M. H. Heemels, and H. Nijmeijer, "Tracking control for hybrid systems with state-triggered jumps," *IEEE Transaction on Automatic Control*, vol. 58, no. 4, pp. 876–890, 2013.

[4] A. Saccon, N. van de Wouw, and H. Nijmeijer, "Sensitivity analysis of hybrid systems with state jumps with application to trajectory tracking," in *53rd IEEE Conference on Decision and Control*, Los Angeles, USA, December 2014, pp. 3065–3070.

[5] J. Biemond, W. Heemels, R. Sanfelice, and N. van de Wouw, "Distance function design and Lyapunov techniques for the stability of hybrid trajectories," *Automatica*, vol. 73, pp. 38–46, 2016.

[6] L. Menini and A. Tornambè, "Asymptotic tracking of periodic trajectories for a simple mechanical system subject to nonsmooth impacts," *IEEE Transactions on Automatic Control*, vol. 46, no. 7, pp. 1122–1126, 2001.

[7] J. Grizzle, C. Chevallereau, R. Sinnet, and A. Ames, "Models, feedback control, and open problems of 3d bipedal robotic walking," *Automatica*, vol. 50, no. 8, pp. 1955–1988, 2014.

[8] M. W. L. M. Rijnen, A. Saccon, and H. Nijmeijer, "On optimal trajectory tracking for mechanical systems with unilateral constraints," in *54th IEEE Conference on Decision and Control*, Osaka, Japan, December 2015, pp. 2561–2566.

[9] G. Incremona, A. Saccon, A. Ferrara, and H. Nijmeijer, "Trajectory tracking of mechanical systems with unilateral constraints: Experimental results of a recently introduced hybrid PD feedback controller," in *54th IEEE Conference on Decision and Control*, December 2015, pp. 920–925.

[10] M. W. L. M. Rijnen, A. van Rijn, H. Dallali, A. Saccon, and H. Nijmeijer, "Hybrid trajectory tracking for a hopping robotic leg," in *6th IFAC International Workshop on Periodic Control Systems*, Eindhoven, The Netherlands, June 2016, pp. 1–6.

[11] J. Salini, V. Padois, and P. Bidaud, "Synthesis of complex humanoid whole-body behavior: A focus on sequencing and tasks transitions," in *Robotics and Automation (ICRA), 2011 IEEE International Conference on*, 2011, pp. 1283–1290.

[12] K. Bouyarmane and A. Kheddar, "Humanoid robot locomotion and manipulation step planning," *Advanced Robotics*, vol. 26, no. 10, pp. 1099–1126, 2012.

[13] F. Nori, S. Traversaro, J. Eljaik, F. Romano, A. Del Prete, and D. Pucci, "iCub Whole-Body Control through Force Regulation on Rigid Non-Coplanar Contacts," *Frontiers in Robotics and AI*, vol. 2, 2015.

[14] S. Kuindersma, R. Deits, M. Fallon, A. Valenzuela, H. Dai, F. Permenter, T. Koolen, P. Marion, and R. Tedrake, "Optimization-based locomotion planning, estimation, and control design for the atlas humanoid robot," *Autonomous Robots*, vol. 40, no. 3, pp. 429–455, 2016.

[15] B. Henze, M. A. Roa, and C. Ott, "Passivity-based whole-body balancing for torque-controlled humanoid robots in multi-contact scenarios," *The International Journal of Robotics Research*, 2016.

[16] A. Hereid, E. A. Cousineau, C. M. Hubicki, and A. D. Ames, "3d dynamic walking with underactuated humanoid robots: A direct collocation framework for optimizing hybrid zero dynamics," in *2016 IEEE International Conference on Robotics and Automation (ICRA)*, 2016, pp. 1447–1454.

[17] G. Schultz and K. Mombaur, "Modeling and optimal control of human-like running," *IEEE/ASME Transactions on Mechatronics*, vol. 15, no. 5, pp. 783–792, 2010.

[18] B. Brogliato, *Nonsmooth Mechanics. Models, Dynamics and Control*, 2nd ed. Berlin: Springer, 1999.

[19] E. de Mooij, "Hybrid trajectory tracking for impact motions of humanoid robots," Eindhoven University of Technology, Eindhoven, Tech. Rep., June 2016, http://repository.tue.nl/855019.

[20] G. Nava, F. Romano, F. Nori, and D. Pucci, "Stability Analysis and Design of Momentum-based Controllers for Humanoid Robots," in *2016 IEEE/RSJ International Conference on Intelligent Robots and Systems*, Oct 2016.

[21] F. Romano, "Whole-body Torque Control of Underactuated Free-Floating Mechanical Systems," Ph.D. dissertation, iCub Facility, Fondazione Istituto Italiano di Tecnologia, 2016, https://francesco-romano.github.io/docs/romano-phd-thesis.pdf.